International Journal of Heat and Mass Transfer 86 (2015) 519–530

Contents lists available at ScienceDirect

International Journal of Heat and Mass Transfer

journal homepage: www.elsevier.com/locate/ijhmt

Heat and mass transfer mechanisms of a self-sustained thermally driven oscillating liquid–vapour meniscus

Manoj Rao [a], Frédéric Lefèvre [a], Sameer Khandekar [b,*], Jocelyn Bonjour [a]

[a] CETHIL UMR5008, Université de Lyon, CNRS, INSA-Lyon, Univ. Lyon 1, F-69621, Villeurbanne, France
[b] Department of Mechanical Engineering, Indian Institute of Technology Kanpur, Kanpur 208016, India

ARTICLE INFO

Article history:
Received 2 December 2014
Received in revised form 22 February 2015
Accepted 6 March 2015
Available online 28 March 2015

Keywords:
Pulsating heat pipe
Oscillating meniscus
Liquid film drainage
Evaporation
Condensation
Contact line dynamics
Modelling

ABSTRACT

Self-sustained thermally-induced oscillations of a meniscus in a two-phase system, consisting of a liquid plug and a vapour bubble in a capillary tube, are studied. This system represents the simplest 'unit-cell' version of a pulsating heat pipe (PHP). An experimental setup has been built to visualise and record the meniscus oscillations and the thin liquid film that is laid on the wall when the meniscus leaves the evaporator. The pressure and temperature of the vapour are also simultaneously measured. When the temperature difference between the heat source and the heat sink increases, different meniscus dynamics, having excellent repeatability, is observed. The experimental results clearly demonstrate that evaporation of the liquid film is responsible for these patterns. The different components of evaporation and condensation processes are critically analysed. Two different modes of evaporation are observed inside the system: one at the triple-line and one at the liquid–vapour interface. Considering that no comprehensive model of PHP system is available, the conclusions and directions provided in this study are important for building a broader understanding.

1. Introduction

A pulsating heat pipe (PHP) is essentially a passive two-phase heat transfer device, which also belongs to a special category of wickless heat pipes [1,2]. From a technological point of view, this thermal transport system is very simple and can be considered as almost costless [1] compared to other heat transport devices. Therefore, research on PHP as a system has been a point of interest in the recent past and its potential applications in many passive heat transport situations has been extensively studied [3–7]. However, in contrast to large availability of system level studies on PHPs in the literature, the nuances of its operating principles and associated physics are not well understood, which thwarts the large scale industrial acceptability of PHPs.

A PHP consists of a simple capillary tube, with no wick structure, bent into many turns, and partially filled with a working fluid. When the temperature difference between the heat source and the heat sink exceeds a certain threshold, the vapour bubbles and liquid plugs present inside the capillary tube begin to auto-oscillate, back and forth, which leads to unique heat transfer characteristics. Heat is thus passively transferred, not only by latent heat exchange like in conventional heat pipes, but also by sensible heat transfer between the wall and the fluid. This complex internal thermo-hydrodynamic transport process is known as the self-sustained thermally driven oscillating two-phase Taylor bubble flow.

Research on PHPs has seen an unprecedented increase during the last 15 years, almost 25 years after the system has been patented in its most popular layout by Akachi [8,9]. Unfortunately, major part of the literature does not provide universally applicable generic knowledge base on these systems; it generally focuses on one particular PHP structure or type, designed for a specific application. In these type of works having a system level approach, the PHP is usually characterised by the temperature difference measured between the condenser and the evaporator section, for a given applied heat flux. Every such PHP design has its own geometrical and thermophysical properties (inner and outer diameters, length, closed or open-loop devices, evaporator, condenser and adiabatic lengths, number of turns, material of the tube, etc.) and is filled with a specific working fluid having its own thermophysical properties (latent heat, wettability and for both vapour and liquid phases: thermal conductivity and capacity, density, viscosity, etc.), and is tested in specific experimental conditions (heat load at the evaporator, ambient and condenser temperatures, etc.). The number of relevant parameters to characterise a PHP is therefore so large that it is difficult to

* Corresponding author.
E-mail address: samkhan@iitk.ac.in (S. Khandekar).

http://dx.doi.org/10.1016/j.ijheatmasstransfer.2015.03.015
0017-9310/

Nomenclature

$\hat{a}$	average acceleration of meniscus (m/s^2)
Bo	Bond number ($\rho \cdot \hat{a} \cdot D^2/\sigma$)
Ca	Capillary number ($\mu U/\sigma$)
D	diameter (m)
h	heat transfer coefficient (W/m^2 K)
h_{lv}	latent heat (J/kg)
K	thermal conductance (W/K)
L	length (m)
m	mass (kg)
$\dot{m}$	mass flow rate (kg/s)
$\overline{M}$	molecular weight (kg/mol)
P	pressure (Pa)
R	radius (m)
$\bar{R}$	universal gas constant (J/mol K)
t	time (s)
T	temperature (°C or K)
x	coordinate (m)
U	velocity (m/s)
V	volume (m^3)

Greek symbols

δ	film thickness (m)
λ	thermal conductivity (W/m K)
μ	dynamic viscosity (Pa-s)
ρ	density (kg/m^3)
σ	surface tension (N/m)

Subscripts

a	adiabatic
c	condenser
$cond$	condensation
e	evaporator
f	film
i	internal
l	liquid
max	maximum
sat	saturation
v	vapour
0	initial

explicitly discriminate the effect of one parameter among the others in this type of experiments. As a result, one can find several papers [1] dealing with the same parameters and often having conflicting or repetitive conclusions. To overcome these difficulties, some authors developed non-dimensional expressions based on different numbers like the Jacob, the Karman, the Prandtl or the Kutateladze numbers and taking into account the number of turns [10]. Nevertheless, this approach has also failed so far to provide a universal understanding of the PHP because the basic physical phenomena and the extent of parameters responsible for system dynamics are not yet well understood.

Research at the local scale (i.e., at the scale of one bubble and one liquid plug), although few, were addressed quite early, in order to augment the knowledge on basic phenomena which are responsible for the oscillations and the heat transfer in the system. From a modelling perspective, this approach was initiated by Zhang et al. [11,12] and Dobson [13,14], who studied theoretically the governing mechanisms of a single branch of the PHP, consisting of one vapour bubble and one liquid slug. Das et al. [24] developed a more sophisticated approach which included the two-phase equilibrium physics that occurs locally at the liquid vapour-interface, especially along the time-varying wetting thin film. Such a film gets laid down by the liquid plug during its journey from the evaporator towards the condenser and through which the major part of heat and mass transfer occurs. This film was shown to be one of the major phenomena responsible for the large amplitude oscillations observed in the system. In this work, an instability analysis of this system was also performed. The local scale modelling has now been extended to several PHP branches with many liquid plugs and vapour bubbles [15–19].

Looking at the literature related to experimental studies on PHPs, the local approach to study its characteristics is comparatively even scarcer. Local heat transfer measurements in non-boiling Taylor bubble flow, in the context of pulsating heat pipes have been recently addressed. Many research groups have shown that the flow field in single-phase liquid flows gets significantly modified by slipping Taylor bubbles of gas/vapour through it, which eventually leads to enhanced heat transfer [20–22]. Continuing on these lines, Mehta and Khandekar [23] recently studied the heat transfer characteristics of pulsating Taylor bubble-train flow in square mini-channels using infra-red thermography, the frequency of imposed flow fluctuations being similar to those encountered in PHPs. The main objective of the study was to observe the effects of externally imposed pulsations on local heat transfer taking place in a unit cell, comprising of a Taylor liquid slug trapped between two adjacent gas bubbles. The controlling parameter of the study was liquid and gas flow rates and imposed flow frequencies. The study indicated that the distribution of liquid-slugs and vapour bubbles is one of the important parameter for improving thermal performance of PHPs. Perturbing the Taylor bubble-train flow with imposed frequencies may conditionally lead to enhancement in the heat transfer, in comparison to steady continuous Taylor bubble-train. The sensible heating/cooling transport capability of the liquid slugs can be altered by controlling the wake generated by the adjoining Taylor bubbles. Interfacial slip created by intermittent flow conditions, was the major cause for heat transfer enhancement.

Earlier, in 2010, Das et al. [24] presented the first experimental data of the simplest 'unit-cell' version of a pulsating heat pipe, consisting of one liquid plug and one vapour bubble. Their experimental setup was closer to a real-PHP and also, the theoretical configuration previously studied by Dobson [13,14]. It consisted of a capillary tube closed at one end and connected to a reservoir maintained at a constant pressure at the other end. A single liquid plug adjoining a vapour bubble was made to thermally auto-oscillate inside this tube, which was heated on one side and cooled down on the other side, thereby creating a continuous cycle of evaporation and condensation. The movement of the meniscus was recorded in the cooled section of the tube, while the heated section, made of copper, was opaque. The vapour pressure was also measured during the oscillations. A similar experiment performed in cryogenic conditions was presented by Bonnet et al. [25] in 2011 and Gully et al. [26] in 2013. Compared to the previous experiment, their system was totally opaque; a thin micro-thermocouple was used to measure the time-varying temperature of the vapour, which showed that the vapour plug is superheated in this single branch PHP experiment. This is a major result as this hypothesis had never been verified before, although it was proposed earlier by Khandekar et al. [27]. Some important experimental limitations were present in the work of Das et al. [24]. The experimental setup

was not fully transparent, except the condenser section as indicated earlier, and therefore the internal hydrodynamic phenomena could not be observed in totality. Besides, the connection between the opaque metal evaporator and the glass condenser section, presented minor flow perturbations having potential impact on the smooth meniscus movement to a certain extent. Furthermore, experiments were done without any synchronization of the internal pressure measurements with the videography.

In 2013, Rao et al. [28] made the pressure measurements in the evaporator section, fully synchronized in real-time with the high speed videography camera. This singular improvement of the setup led to a drastic improvement in the overall understanding of the complex liquid film evaporation and ensuing pressure fluctuations inside the unit-cell. Contrary to obvious interpretations, maximum pressure in the vapour bubble was achieved in the downward stroke of the meniscus, rather than its upward stroke. Thus, it was concluded that the system dynamics cannot be compared with gas-compression cycles; the presence of vapour, coupled with transient phase-change processes, give rise to unique transport phenomena. In this paper, new experimental data are presented using the same experimental bench of Rao et al. [28]. A second high speed camera is used to record the evaporation of the wetting film laid down by the meniscus when it leaves the evaporator. The captured temporal data enable to bring some very useful information and perspective to characterise the heat and mass transfer mechanisms of a self-sustained thermally driven oscillating two-phase system, such as a PHP. The different components of evaporation and condensation processes inside the system are critically analysed. Two different modes of evaporation are observed inside the system: one at the triple-line and one at the liquid–vapour interface. The dynamics of the thin film is theoretically described using the mass and energy balance equations coupled to the experimental data. This new information is vital for furthering the development of a realistic and comprehensive PHP mathematical model.

2. The ‘unit-cell’ experiment

The experimental set-up is presented in Fig. 1. As noted, it is an improved version of a previous experimental design presented by Das et al. [24] and further used by Rao et al. [28]. It mimics the basic unit-cell of a PHP, with one liquid plug and one vapour bubble, located in a vertical capillary tube of circular cross-section. The transparent capillary tube of inner diameter 2.0 mm, made of glass, is closed at one side and connected to a reservoir maintained at a constant pressure at the other side. The liquid plug oscillates between a heat source located near the upper closed side (length L_e = 20 cm) and a heat sink located near the bottom reservoir (length L_c = 20 cm). In between, a small adiabatic section of length L_a = 1 cm separates the heat source and the heat sink. In the following, the heat source and the heat sink will often be termed ‘evaporator’ and ‘condenser’, from an analogy with conventional heat pipes. One should however be aware that strictly speaking, this terminology is not fully adequate in the present system, since condensation can also occur in the evaporator as it has been shown earlier by Rao et al. [28] too, and further corroborated by the results of the present study.

The evaporator and the condenser are transparent heat exchangers, whose temperature is controlled by two thermostatic baths with an overall accuracy of ±1 °C. A third thermostatic bath is used to control the temperature of the reservoir (±0.2 °C), and thus its saturation pressure. The two-phase oscillatory flow is characterised by vapour pressure measurements as well as meniscus displacement measurements. An absolute pressure sensor (supplied by Kistler®, piezo-resistive sensor type 4007B, operating range of 0–5 bar, accuracy ±0.1% of full-scale reading) is located at the closed end of the tube. Two high speed cameras (Photron-Fastcam® 1024-PCI and SA-3, respectively) are simultaneously used to record the meniscus displacement and movement of the triple-line. A K-type thermocouple of diameter 80 μm is also inserted from the top of the capillary tube to measure the temperature of the vapour, as shown. The pressure and temperature measurement is synchronized with the two video cameras with external trigger. Before the experiments, the system is completely evacuated to remove the non-condensable gases using a vacuum pump ($<10^{-5}$ mbar). The reservoir is then filled with the working fluid, i.e., FC72. The volume of the liquid reservoir is exceedingly large as compared to that of the capillary tube. This ensures that any internal meniscus oscillations have a negligible effect on the reservoir static pressure. The capillary tube always remains dipped inside the liquid irrespective of level of the liquid meniscus in it during

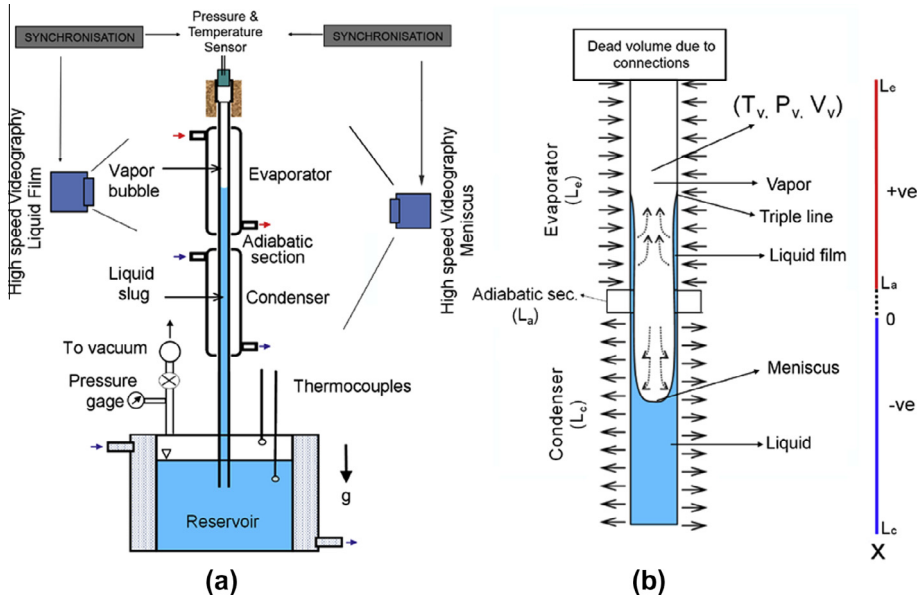

Fig. 1. (a) Schematic of the experimental set-up for obtaining self-sustained thermally driven oscillating flow of a ‘unit-cell’ consisting of one vapour bubble and one liquid plug. (b) Details of the unit-cell highlighting the characteristic lengths and relevant parameters.

the experiment. The change in liquid level affects the hydrostatic pressure at the outlet of the tube, but in third place of decimal, as the height of liquid above the tube exit is designed to be lower than 100 mm.

2.1. Results and discussion

Experimental results are discussed for various operating boundary conditions. The reservoir is maintained at a constant pressure of 0.5 bar, corresponding to a saturation temperature of 37.2 °C. The evaporator temperature T_e is kept constant at 46 °C while the condenser temperature T_c is varied from 0 to 32 °C. It is observed that when T_c is kept below 16 °C (large temperature difference between the evaporator and condenser) or above 28 °C (low temperature difference between the evaporator and condenser) the meniscus moves rather randomly and hence, it is very hard to obtain repeatability in results. For the condenser temperature in between 16 and 28 °C systematic and repeatable oscillations of pressure and meniscus movement are observed. Therefore, the results presented in the next sections are taken in this range to arrive at meaningful conclusions which can contribute in attaining the objectives of this research.

2.1.1. Meniscus oscillation with pressure variation

Fig. 2 shows the temporal variation of vapour pressure in the vapour bubble, along with the location of the meniscus and the triple-line, for four cases of the experimentally applied boundary conditions (T_e = 46 °C and T_c = 16, 20, 24 and 28 °C, respectively). The location x = 0 corresponds to the bottom of the adiabatic section. Locations defined by $x > L_a$ are in the evaporator section while those defined by $x < 0$ are in the condenser section. Three complete meniscus motion cycles are presented for each condenser temperature. It is observed that meniscus movement and pressure variation are quasi-periodic and nicely repeatable for all of the cases. When the meniscus moves towards the condenser (downward motion), a thin liquid film gets drained or laid on the tube wall. As it will be explained later, this film drainage by the moving meniscus is responsible for the large amount of vapour generation at the evaporator, which, in turn, leads to the oscillation of the liquid plug.

By looking at the video of meniscus motion, it is possible to distinctly observe three different zones inside the tube: a dark zone corresponding to the liquid plug, a clear zone corresponding to the vapour slug, and an in-between zone where the contrast is neither dark nor clear that corresponds to this thin liquid film, which gets laid down during meniscus downward motion. Furthermore, under proper lighting conditions and controlled focus, it is also possible to clearly observe the liquid film vanishing with time, i.e., evaporation of the film from the glass surface is unmistakably recorded. The movement of the triple-line towards the condenser is also clearly observable. We consider that the liquid film vanishes when the contrast value observed on the video is similar to the contrast value due to the vapour. However, as the contrast depends on the thickness of the liquid film, the sensitivity of the camera is probably not able to distinguish film-remnants which are extremely thin. Therefore, subsequent analysis is based till the location where the difference of contrast is just vanishing. However, one should keep in mind that the absence of explicit quantitative data points does not mean with certainty that the liquid film has indeed totally vanished; a few monolayers of liquid may still be remaining. Nevertheless, the recorded information certainly enables to bring some essential information for qualitative interpretations.

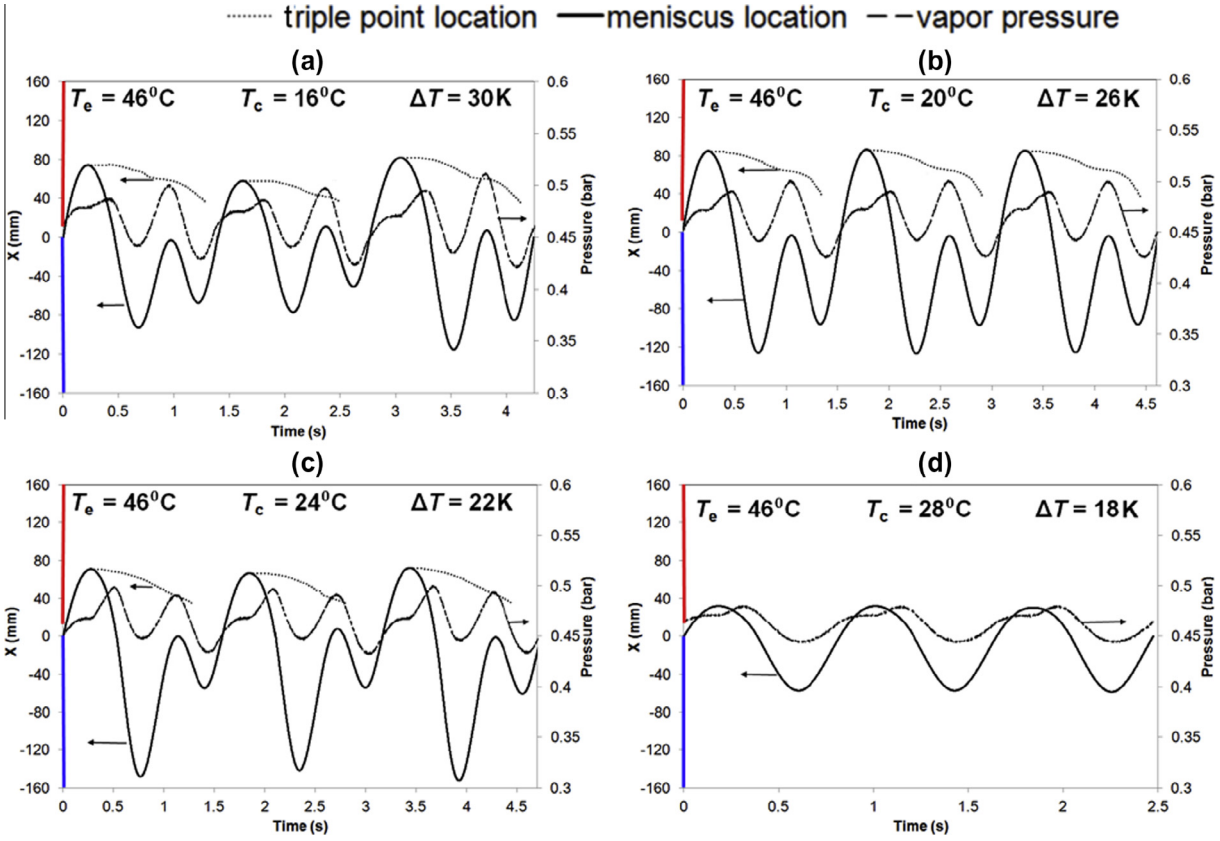

Fig. 2. Temporal variations of pressure (right ordinate axis) in the vapour bubble along with location of meniscus (left ordinate axis, solid line) and triple-line (left ordinate axis, dotted line) for experimental condition of T_e = 46 °C and (a) T_c = 16 °C, (b) T_c = 20 °C, (c) T_c = 24 °C and (d) T_c = 28 °C.

For T_c = 16 °C (Fig. 2a), T_c = 20 °C (Fig. 2b) and T_c = 24 °C (Fig. 2c), the meniscus cycle consists of one full stroke inside the evaporator followed by two smaller strokes in the condenser section. During the downward stroke of the meniscus, as noted earlier, it lays down a thin liquid film. Evaporation of this film adds mass to the vapour space and helps in increasing the vapour pressure. Until the time the liquid film laid down by the downward moving meniscus is completely evaporated, the meniscus is not able to re-enter the evaporator, and thus moves back again twice into the condenser. Thus, two strokes are seen to occur in the condenser section. The meniscus re-enters the evaporator section, after the second stroke in the condenser is over, and then the quasi-periodic cycle continues. The maximum high level reached by the meniscus inside the evaporator is rather constant and close to x = 80 mm for the different condenser temperatures. This tends to suggest that the amount of vapour generated during one cycle at the evaporator is rather constant, since it is proportional to the length of the liquid film drained by the meniscus in the evaporator. Conversely, the maximum level reached by the meniscus inside the condenser increases with the increase of T_c during the first stroke inside the meniscus. Indeed, for smaller condenser temperatures (larger temperature difference), a smaller heat exchange surface area is necessary to condense the vapour generated by the evaporation of the liquid film. The second stroke in the condenser is always shorter than the first one, which can be explained by a smaller amount of vapour generated in the evaporator (the last remnant of the disappearing liquid film), as the remaining liquid film length is much smaller at the end of a cycle. One can also observe that the cycle time-period slightly increases with the increase of T_c.

The qualitative behaviour of the meniscus oscillatory motion is quite different for T_c = 28 °C; the meniscus oscillation cycle consisting of a single to-fro stroke in the evaporator, followed by one stroke in the condenser section. Therefore, the net time period of one oscillation cycle is also smaller than for the other condenser temperatures. One can also observe that the amplitude of the signal is much smaller in both the condenser and the evaporator. Above a condenser temperature of 28 °C, the energy of the system is not sufficient to maintain the oscillations. It was not possible to distinguish clearly the triple-line evaporation in that case because the length of the film formed due to drainage was very short, compared to other condenser temperatures. Lastly, comparing the pressure signal for the four graphs (Fig. 2a–d), shows the decrease of its amplitude with the decrease of the difference between T_e and T_c. The maximum of amplitude varies from 0.16 to 0.06 bar, when T_c varies from 16 to 28 °C, respectively.

The oscillatory behaviour of the meniscus can be directly and definitely linked with the nature of the liquid film laid by the meniscus while coming down from evaporator. This phenomenon is explained with details in Fig. 3, where the boundary conditions are T_e = 46 °C and T_c = 20 °C. Time evolution of the meniscus from the evaporator (Stage A), as it passes towards the condenser (Stage J) and comes back to the evaporator (Stage T), is shown. Fig. 3b is a typical temporal variation of pressure in the vapour bubble and movement of triple-line depicting several steps of the meniscus motion along with different stages in one cycle (A to T).

From points A to E, the meniscus is moving upwards in the evaporator and is in the process of approaching the top-most position in the evaporator. During that stage, the vapour space is getting compressed and the pressure of the vapour bubble is simultaneously increasing. At point E, the meniscus reaches the topmost position of evaporator and dwells there for a very short time. This dwelling can be observed both in meniscus location and pressure variations (Fig. 3b). After point E, the meniscus starts its downward journey. It is observed that a film of liquid is laid on the wall of the tube and the triple-line location coincides with point E. As the meniscus starts moving downwards, this triple-line also starts following it but with a different speed. At point J, the meniscus is about to exit from the evaporator, as it enters the condenser section. It is clearly visible in the figure that at this stage the liquid film still exists in the evaporator section. As it was already described in Rao et al. [28], the maximum value of vapour space pressure is not reached when the meniscus is at its topmost location in the tube, but just before it enters into the condenser. Indeed, evaporation of the liquid film during the downward movement of the meniscus towards the condenser contributes to the increase of the pressure during the descent of the liquid plug.

From points K to M, the meniscus keeps on moving downwards in the condenser and the pressure begins to decrease, due to both, expansion of the vapour bubble and simultaneous condensation. At point M, the meniscus reaches the first bottom-most point in the condenser. The liquid film, albeit thinner, is still in the evaporator. From point N to point P, the vapour-pressure still decreases, and the meniscus moves towards the evaporator. During this upward motion of the meniscus in the condenser section, the pressure increases again, clearly indicating that the rate of vapour condensation process is not sufficient to overcome the mass addition rate due to the evaporation of the remaining liquid film. Therefore, the meniscus is not able to reach the adiabatic section, but changes its direction to move downwards again instead of entering the evaporator. This, as explained, happens due to the continued presence of the liquid film in evaporator, which is still continuously evaporating, thus restricting the upward motion of the meniscus. From points P to R the meniscus again re-travels till the bottom-most point of the condenser and very quickly thereafter, the vapour pressure decreases again. Meanwhile, no sooner the liquid film vanishes in between point R to T in the evaporator, subsequent variation of the mass of vapour is only due to condensation and therefore the pressure of the vapour decreases until a very low value that enables the meniscus to be pulled up into the evaporator section yet again. This process then repeats itself, starting from A to T, with regular repeatable cyclic oscillations.

As has been appreciated, during one complete cycle of meniscus motion, the variation of the vapour pressure is due to both, evaporation and condensation of the fluid and compression or expansion phenomena of the vapour. During the ascent of the meniscus in the evaporator (upward stroke), no thin liquid film is present ahead of the meniscus. Hence during this part of the motion, there is practically no mass addition to the vapour space due to evaporation and the pressure change is directly attributable to compression effect, which results in a small variation of the pressure during that stage. This result undoubtedly highlights the importance of the thin film evaporation and vapour condensation phenomena in the ensuing auto-oscillations of the meniscus, as compared the purely compression and expansion effects.

Fig. 3b represents the time-evolution of the meniscus location and corresponding variation of vapour pressure during a period of 1.6 s. In addition, the location of the moving triple-line, i.e., the edge of the liquid film on the channel wall, is also displayed on this figure. It is clearly visible that the liquid film motion always lags behind the meniscus and takes finite time to evaporate. However, as mentioned earlier, it was not possible to record the variation of liquid film thickness until the very end of the evaporation process, due to photographic limitations. Nevertheless, it is clear that the lifespan of the liquid film in the evaporator is rather long as compared to the total time period of the oscillation. Therefore, until the meniscus completes the first part of the cycle of travelling through to the bottom-most point of condenser and then again coming back to the entrance of evaporator, remnants of the evaporating liquid film still exists in evaporator, thereby restricting the entry of the meniscus into evaporator and pushes it back to the condenser. This behaviour of the meniscus movement is responsible for small and big amplitude oscillations, respectively. As soon as the

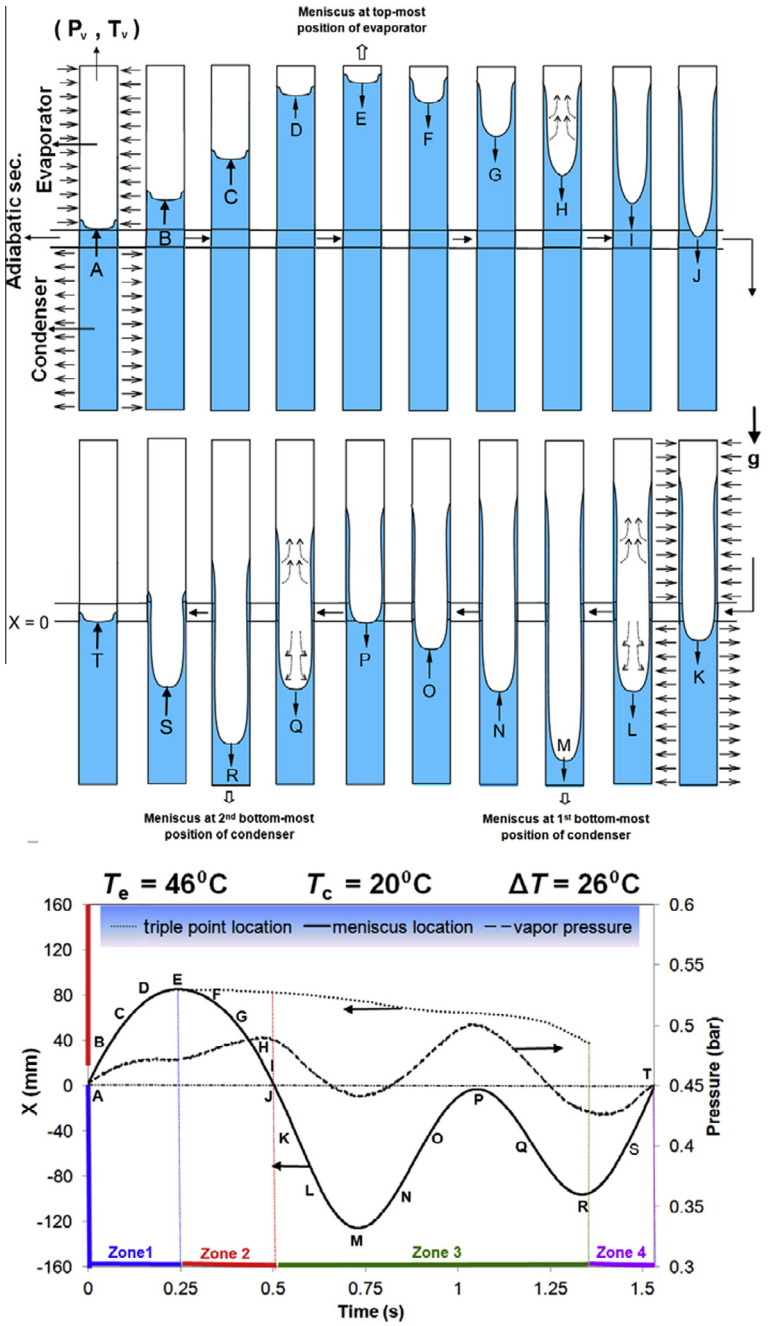

Fig. 3. (a) Schematic explaining the events during one cycle of the meniscus motion. (b) Time evolution of the meniscus from the entrance in the evaporator (Stage A) as it passes towards the condenser (Stage J) and comes back to the evaporator (Stage T), is shown. The four zones, as explained in the text, are also highlighted.

liquid film completely disappears from the evaporator, the meniscus is able to re-enter the evaporator again during its return motion from condenser. In this way, regular and repeatable self-sustained thermally driven oscillations go on in the tube at the imposed thermal gradient. With reference to the Fig. 2, it can be said that the film life, i.e., the time period between the film appearing and subsequently completely getting evaporated and vanishing, is of the order of typically between 1.0 and 1.4 s.

2.1.2. Actual vapour temperature versus the vapour saturated temperature

Fig. 4 presents temporal variations of pressure and temperature in the vapour bubble depicting several cases of the experimentally applied boundary conditions (T_e = 46 °C and T_c = 16, 20, 24 and 28 °C). The saturation temperature of the working fluid corresponding to the measured pressure is also plotted along with the measured vapour temperature. The measurement of temperature by this micro-thermocouple is critical and requires close scrutiny. Indeed, even if the size of the thermocouple is rather small (bead diameter is 80 μm), its frequency response, although much faster than the oscillating frequency of the system, is still finite and non-zero. Furthermore, the micro-thermocouple also exchanges heat by thermal radiation with the inner wall of the capillary tube (although emissivity of both the surfaces is expected to be quite low), which will introduce a non-vanishing bias in the temperature measurement. The precision of the temperature sensor would be lower than ±0.5 K if it was only based on a calibration process, but the previous described experimental biases increase

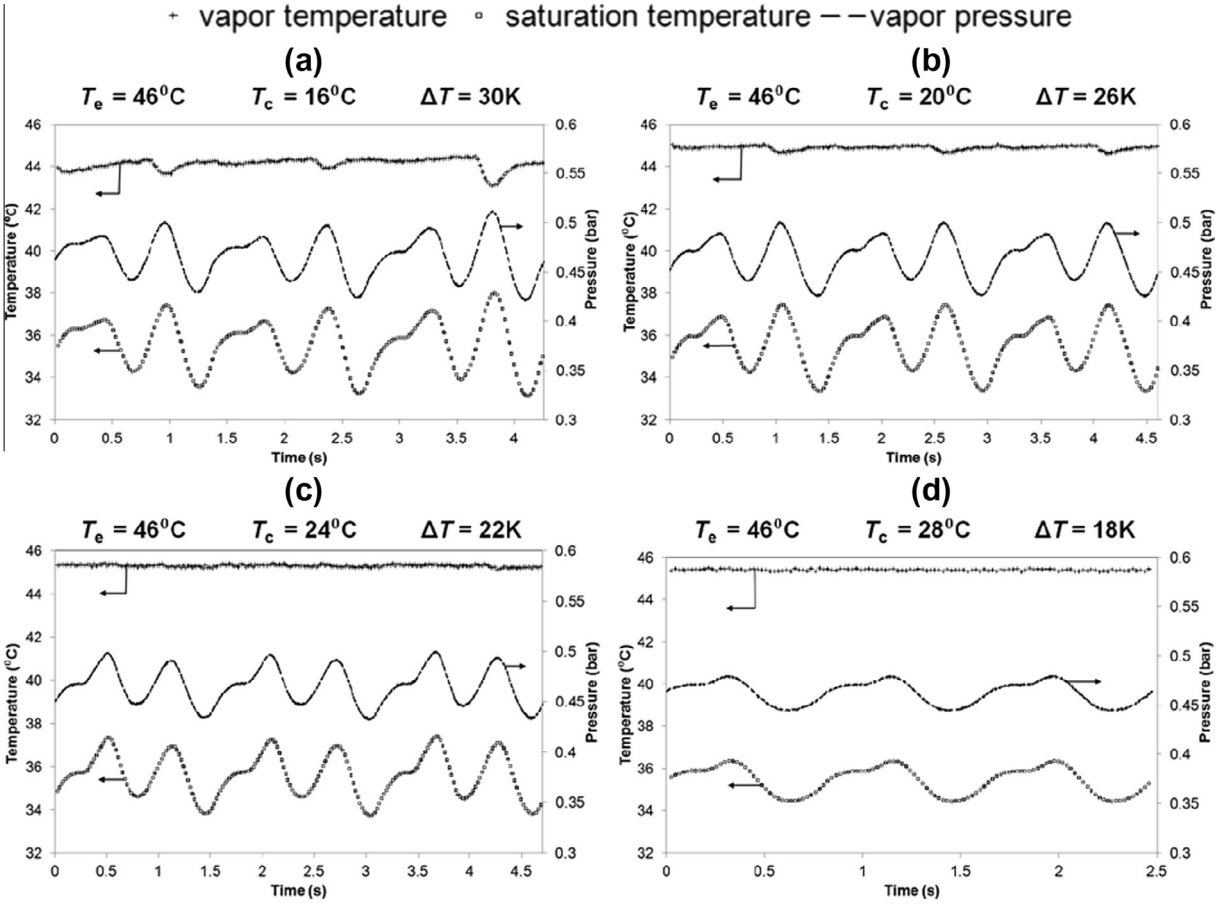

Fig. 4. Temporal variations of pressure (right ordinate axis) along with temperature in the vapour bubble and saturation temperature $T_{sat} = f(P_v)$, for experimental condition of T_e = 46 °C and T_c = 16, 20, 24 and 28 °C, respectively.

this uncertainty and make it difficult to estimate it properly. However, even with these limitations, the temperature information given by this micro-thermocouple provides some very useful information for qualitative interpretations of the system dynamics.

Firstly, it is seen that the measured vapour temperature is somewhat lower than the maintained evaporator temperature. The variation is extremely small, which can be due to the dampening of the signal due to the non-zero time response of the system.

Secondly, and more strikingly, one major conclusion is that the vapour temperature is always higher than the saturated temperature derived from corresponding vapour pressure measurement, which corroborates the recent results obtained by Gully et al. [26] in cryogenic conditions. Their study also brings out the existence of superheated conditions of the vapour space during meniscus motion. This is a quite an important conclusion for the proposed modelling of the unit-cell PHP system. The fact that vapour is seen to be always superheated throughout the cycle of meniscus oscillation provides the first-order justification for using the ideal gas equation for modelling the vapour space, in conjunction with the film dynamics in the evaporator and film condensation in the condenser; the latter two models providing the respective sources and sinks for vapour mass, corresponding to the evaporation and condensation rates, respectively. In the subsequent section, this idealisation is used to find the temporal mass variation in the system, and as will be demonstrated, this exercise does provide important insights into the thermal-fluidic behaviour of self-sustained thermally driven oscillatory meniscus motion.

3. Dynamics of the liquid film

The vapour mass dynamics can be estimated using simple assumption of ideal gas equation and the different measurements made via the sensors placed in the vapour space. This information, coupled to the temporal movement of the triple-line, enables to estimate the time-dependent changes of the liquid film thickness. Finally, a simple mass balance equation in the evaporator provides an estimation of the initial thickness of the film. Hence, the dynamics of the film in the evaporator can be completely derived; this procedure is detailed below.

3.1. Experimental estimation of the vapour mass dynamics

The experiment provides the instantaneous location of the meniscus inside the capillary tube during its oscillatory motion. In other words, the instantaneous volume of vapour $V_v(t)$ can be estimated, neglecting the microscopic volume which the liquid film occupies. The net vapour volume is composed of the volume of vapour inside the tube and a constant dead volume which is due to the connections of measuring instruments. This dead volume has been experimentally determined and is equal to 2.83×10^{-6} m^3 ($\pm 3\%$). To measure this dead volume, the empty weight of the connections (T-junction) which is used to connect the thermocouple and the pressure transducer was measured, with help of a highly precise mass balance. Then, the system is filled with water and the difference of mass is used to calculate the dead

volume inside the system. This process is repeated several times to minimize the error.

The instantaneous pressure of the vapour plug $P_v(t)$ is also known from the measurements. Furthermore, it was shown in the last section that the vapour temperature $T_v(t)$ is always above the saturation temperature. Therefore, ideal gas equation can be invoked to obtain the instantaneous mass of vapour $m_v(t)$ inside the system:

$$m_v(t) = \frac{P_v(t) \times V_v(t)}{\bar{R} \times T_v(t)} \times \overline{M} \tag{1}$$

where $\bar{R}$ is the universal gas constant and $\overline{M} = 338$ g/mol, the molecular weight of FC72.

Fig. 5 shows the temporal variations of meniscus location and triple-line locations, respectively, along with the mass of vapour calculated using ideal gas, Eq. (1), depicting several cases of the applied boundary conditions ($T_e = 46$ °C and $T_c = 16$, 20 and 24 °C). Vapour mass variation inside the system is a combined effect of evaporation and condensation, respectively, which may be occurring simultaneously. Therefore, any combination of evaporation and condensation rates can produce this variation of vapour mass. One has to develop a heat transfer model to extract these parameters from the experimental data. It is also observed in Fig. 5d that even a ±10 °C variation in vapour temperature measurement affects only ±3% of instantaneous vapour mass calculations. Therefore, even if the temperature measurement by the micro-thermocouple is not highly accurate, the validity of the estimation of the vapour mass certainly remains rather reasonable.

To analyse the experimental data, the oscillation cycle is divided into four different zones that are earlier depicted in Fig. 3b. In Zone #1, between points A and E, there is no liquid film on the tube wall as the meniscus is moving up in the evaporator. Simultaneously, we observe a decrease of the mass of vapour that can be explained by condensation on the meniscus due to compression of the vapour. From point E to J, referred to as Zone #2, the meniscus is moving down in the evaporator tube section and is laying a liquid film on the evaporator wall. Hence, the length of the liquid film in the evaporator increases due to the downward movement of the meniscus and decreases due to simultaneous evaporation. Zone #3 commences from Point J onwards and terminates when the liquid film cannot be observed anymore. In this operational zone, it is assumed that the length of the liquid film in the evaporator is only decreasing due to its evaporation at the triple-line. The last zone is Zone #4, where the vanishing liquid film cannot be observed due to the lack of camera resolution. Nevertheless, a few monolayers of liquid film remnants may still remain which will subsequently evaporate. While condensation of vapour occurs primarily on the liquid film in the condenser, it can also be observed on the liquid film in the evaporator, as has also been shown by Rao et al. [28]. Indeed, the temperature of the liquid plug coming from the condenser region and entering into the evaporator section in the upward stroke (A to E) is much lower than the vapour temperature already present there. Since

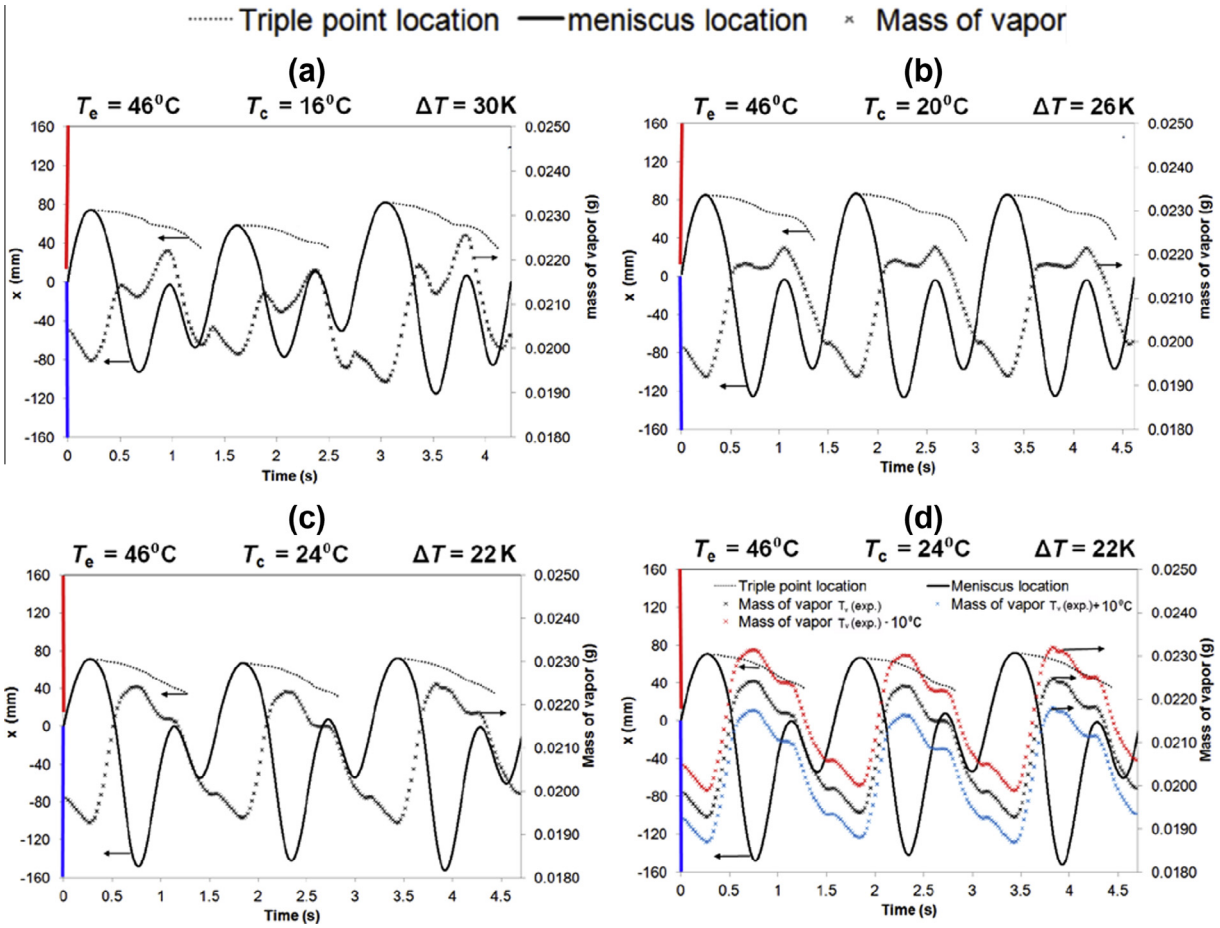

Fig. 5. Temporal variations of location of meniscus (left ordinate axis, solid line), triple-line (left ordinate axis, dotted line) and mass of vapour (right ordinate axis) calculated using ideal gas equation (Ref. Fig. 1) and Eq. (1) (at $T_e = 46$ °C and (a) $T_c = 16$ °C, (b) $T_c = 20$ °C, (c) $T_c = 24$ °C, and (d) $T_c = 24$ °C, respectively, showing the sensitivity of the vapour temperature on the mass of vapour).

diffusion time scales in the bulk liquid region are large, as clearly indicated by Rao et al. [28], the temperature of the liquid film that is laid by the meniscus during its journey towards the condenser is much lower than the adjoining vapour mass, which leads to condensation on the film surface. After a while, the liquid film temperature increases due to heat conduction from the wall. Then, evaporation of the liquid film begins at the liquid vapour interface. All these physical mechanisms have to be introduced in the heat and mass transfer model to understand the dynamics of the liquid film. The mass transfer interactions due to the liquid film at the evaporator section are complex and its understanding is the key to this analysis.

3.2. Modelling vapour mass dynamics

The variation of vapour mass is estimated from the raw experimental data, as per Fig. 5. This variation is due to four different contributions:

- Condensation of vapour on the liquid film portion in the condenser section,
- Condensation of vapour on the meniscus formed between the vapour plug and the liquid slug,
- Evaporation at the triple-line formed between the liquid film, the wall and the vapour phase,
- Mass transfer (evaporation or condensation) between the liquid film and the vapour in the evaporator section.

The condensation rate due to the first two terms can be obtained by the energy equation:

$$\dot{m}_{cond} = \frac{1}{h_{lv}}\left(h_{c,lf}\pi D_i L_{c,lf}(t)[T_{sat}(t) - T_c] + K_{cond}[T_{sat}(t) - T_c]\right) \quad (2)$$

where, K_{cond} is the overall thermal conductance of condensation occurring on the meniscus and $h_{c,lf}$, the condensation heat transfer coefficient between the vapour and the condenser; the justification for taking these two terms separately and their relative importance will be clear in the subsequent analysis which follows. In Eq. (2), T_{sat} is the saturation temperature corresponding to the pressure of the vapour, which will apply at the interface and T_c the temperature of the heat sink, which is controlled by the thermostatic bath. $L_{c,lf}(t)$ is the instantaneous liquid film length in the condenser. In order to simplify the model, we assume that the liquid–vapour interface at the condenser is hemispherical with diameter D_i. In reality, the interface area is somewhat smaller due to the thickness of the film on the wall, but based on present experimental evidence too, we can safely assume that this thickness is negligible as compared to the tube diameter.

The overall thermal conductance of condensation, K_{cond} can be estimated by comparison between the mass of vapour (Eq. (1)) calculated from the experimental data during the upward motion of the meniscus inside the evaporator (Zone #1) and Eq. (2). Indeed, in Zone #1, the vapour mass variation is only due to this term (and therefore, term #1 in Eq. (2) vanishes in Zone #1 from A to E). The heat transfer coefficient for condensation in the condenser section, $h_{c,lf}$ is linked to the thickness of the liquid film and its order of magnitude can be estimated as $\sim\lambda_l/\delta_0$, where λ_l is the thermal conductivity of the liquid and δ_0 is the initial thickness of the film which is a key parameter for discerning the dynamics of the film [24–26,28]. We assume that the variation of the film thickness due to the condensation of the vapour in the condenser is small enough to be neglected; also, the temperature of the wall at the condenser is constant and equal to T_c. The temperature of the liquid plug inside the capillary tube is also taken to be very close to the condenser temperature.

The mass transfer due to the liquid film in the evaporator is more complex and cannot be obtained by the same approach. Two mechanisms have to be taken into account, i.e., the evaporation at the triple-line and the mass transfer at the liquid–vapour interface of the thin film. The temperature of the inner wall of the evaporator cannot be considered as constant, equal to the heat source temperature in this experiment. Indeed, during one cycle, the upper part of the inner tube is always in contact with the vapour plug while the bottom part of the tube is in contact either with vapour or with the liquid film, or with the liquid plug. Furthermore, as the material of the tube is glass, it has a small thermal diffusivity and therefore its time scale is higher than the oscillation period [28]. For all these compelling reasons, the inner temperature of the wall is an unknown function of time and space. Therefore, the modelling of the dynamics of the film cannot be estimated using an evaporating heat transfer coefficient as was possible in the condenser section.

The thickness of the film in the evaporator is varying from a constant value δ_0 – when the meniscus begins its journey towards the condenser – to zero at the end of the cycle. This variation is due to two different phenomena: the evaporation at the triple-line and the mass transfer at the liquid–vapour interface of the film. Let us assume that $\delta(t)$ is not a function of the location inside the evaporator, but only a function of time. This hypothesis is reasonable as the temporal variation of the location of the triple-line is much slower than the temporal variation of the meniscus location. Therefore, the mass transfer rate between the liquid film and the vapour plug can be expressed as:

$$\dot{m}_{lf} = -\rho_l \pi D_i\left[\delta(t)\frac{dx_{lf}(t)}{dt} + L_{e,lf}(t)\frac{d\delta(t)}{dt}\right] \quad (3)$$

where, $x_{lf}(t)$ is the location of the triple-line and $L_{e,lf}(t)$ is the length of the liquid film in the evaporator, which are outputs of the experiments. The minus sign in Eq. (3) is due to the negative sign of the derivative of x_{lf} and δ during evaporation.The mass variation of the vapour can be expressed as:

$$\dot{m}_v = \frac{dm_v}{dt} = \dot{m}_{lf} - \dot{m}_{cond} \quad (4)$$

The mass of vapour is known at each time (Eq. (1)), therefore the variation of the film thickness can be estimated by:

$$\frac{d\delta(t)}{dt} = -\frac{1}{L_{e,lf}(t)}\left[\frac{\dot{m}_v + \dot{m}_{cond}}{\rho_l \pi D_i} + \delta(t)\frac{dx_{lf}(t)}{dt}\right] \quad (5)$$

Finally, the equation of $\delta(t)$ can be written as:

$$\delta(t) = \delta_0 + \frac{d\delta(t)}{dt}\Delta t \quad (6)$$

This model enables to estimate the complete dynamics of the liquid film by comparison with the experimental data. The initial thickness δ_0 can be calculated by integrating the mass balance equation for the liquid film over a complete period of time:

$$\int \dot{m}_{lf} = \int \dot{m}_v + \dot{m}_{cond} = \rho_l \pi D_i \delta_0 L_{lf,max} \quad (7)$$

One can note that even if one part of the triple-line is not recorded by the high speed camera, Eq. (7) enables to estimate the initial value of δ.

3.3. Comparison of model predictions with experiments

Fig. 6 shows temporal variation of the location of meniscus/triple-line and the film thickness calculated using the described model, for different boundary conditions (keeping T_e = 46 °C constant and T_c varying from 16, 20 and 24 °C, respectively). The mean initial liquid film thickness is estimated to be equal to 75, 69 and

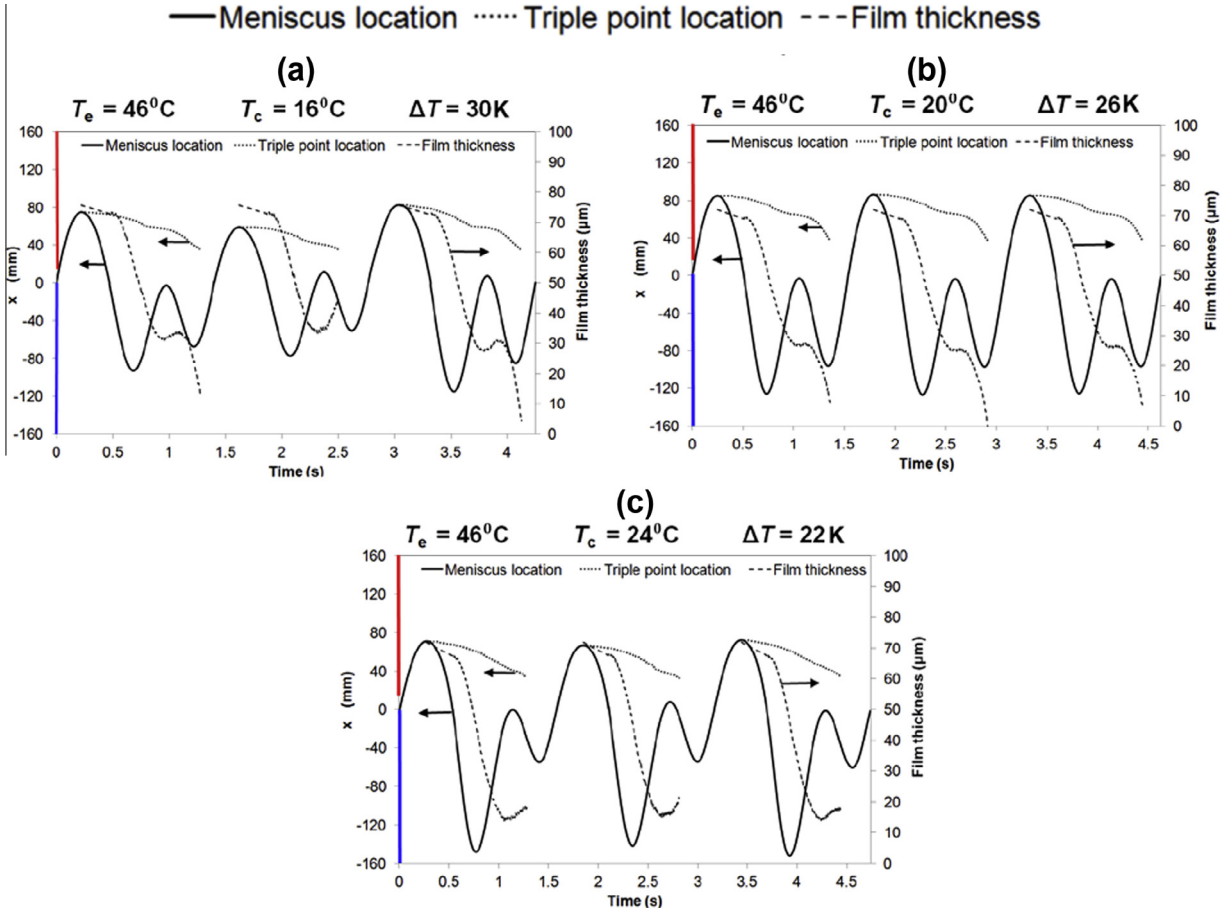

Fig. 6. Temporal variations of location of meniscus and film thickness variation calculated using the analytical model as per Eq. (7) (at T_e = 46 °C and T_c = 16, 20 and 24 °C, respectively).

67 μm for T_c equal 16, 20 and 24 °C, respectively. The thickness is nearly constant in Zone #2, while at the same time, the triple-line moves towards the condenser; this clearly indicates that two different processes of evaporation occur inside the system, one at the triple-line and the other at the liquid–vapour interface of the liquid film. In Zone #3, the liquid film thickness in the evaporator section decreases rapidly as the meniscus recedes deep into the condenser section towards the reservoir. When the meniscus reaches back to the evaporator section during its first upwards journey, a small increase of the film thickness is observed in some conditions, which is attributed to condensation of compressed vapour on the film. In Zone #4, the thickness of the film cannot be estimated as the location of the triple-line is not recorded. Nevertheless, the extrapolation of the thickness profile shows that it decreases to zero when the meniscus enters the evaporator in the next cycle.

The initial film thickness estimated by the model described above in Section 3.2 can also be independently verified by empirical scaling correlations available in the literature; four such correlations are compiled and compared by Khandekar et al. [2]. These correlations predict the initial thickness of liquid film laid down on a wall by a moving meniscus as a function of the Capillary number (defined as $Ca = \mu U/\sigma$) under adiabatic conditions. While most correlations are applicable to steady motion of the meniscus of wetting fluids at low Capillary numbers, Han and Shikazono [29] have developed a correlation for a meniscus moving with a constant acceleration also. The effect of the Bond number (defined as $Bo = \rho \cdot \hat{a} \cdot D^2/\sigma$), is also accounted for in this correlation, which is given as:

$$\frac{\delta_0}{R} = 2 \cdot \left(\frac{0.968 Ca^{2/3} \cdot Bo^{-0.414}}{1 + 4.838 Ca^{2/3} Bo^{-0.414}} \right) \tag{8}$$

The assumptions and conditions under which the above correlation was developed by Han and Shikazono et al. [29] is probably the closest which we can get from the literature, to the conditions of the present experiments. Needless to say, the assumption of adiabatic flow and constant meniscus acceleration are not applicable to the present experiments. However, as will

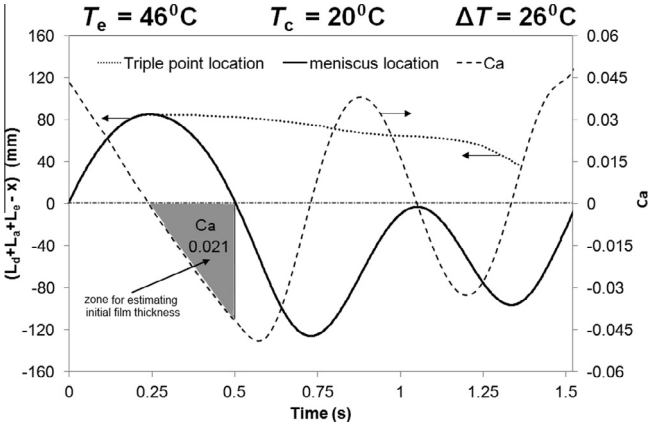

Fig. 7. Variation of capillary number of the meniscus motion during one complete oscillation cycle.

be demonstrated, application of Eq. (8) does provide reasonable order-of-magnitude comparison of the initial film thickness laid down by the downward moving meniscus in the evaporator section.

For demonstrative purpose, the time varying Capillary number of the oscillating meniscus in the present experiment is plotted for one complete cycle (for $T_e = 46$ °C and $T_c = 20$ °C) in Fig. 7. Fig. 8 compares the classical correlations of estimating the film thickness, including Eq. (8); the correlations are noted on the figure itself. As can be observed, all the correlations are fairly consistent with each other. The most appropriate region to apply Eq. (8) is when the meniscus commences its downward journey, laying the thin liquid film in the evaporator section. In this zone, as marked by the shaded gray area in Fig. 7, the average value of *Ca* is 0.021. With average value of *Bo* = 1.72 in this zone, the initial film thickness estimated by Eq. (8) comes out to be equal to ~90 μm. This is within reasonable range of what was earlier predicted by the model described in Section 3.2, i.e., ~69 μm. Table 1 compares the value of the initial film thickness, as obtained by Eq. (8) and the model described in Section 3.2, for the other two boundary conditions of T_e and T_c used in the present work. As noted earlier, given the limitations of assumptions under which the empirical correlations were developed, and the fact that Eq. (8) has itself an accuracy of ±15% (Han and Shikazono et al. [29]), it is encouraging to find that reasonable estimates of the initial film thickness can be independently verified, as can be clearly seen in Table 1.

Fig. 9 presents the four different explicit contributions to the vapour mass variation during one complete cycle ($T_e = 46$ °C and $T_c = 16$ °C). Qualitatively similar results are obtained for the other boundary conditions also. The mass due to condensation on the meniscus region is varying nearly linearly because the vapour saturation temperature, which exists on the meniscus, does not vary much during the experiment and therefore, the difference between T_{sat} and T_c remains nearly constant (see Eq. (2)). In any case, the amount of condensation on the meniscus is negligible compared

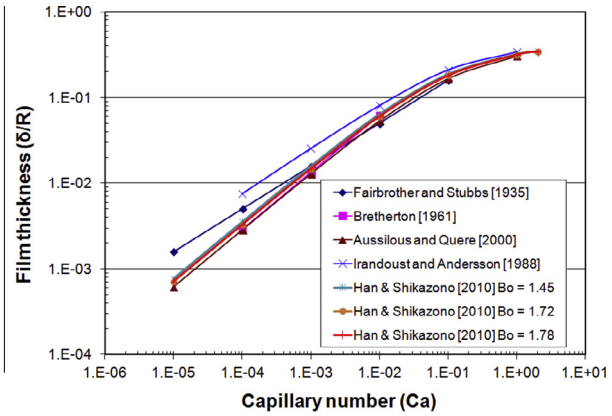

Fairbrother and stubbs [1935]

$$\frac{\delta}{R} = 0.50(Ca)^{1/2}$$

Irandoust and Andersson [1988]

$$\frac{\delta}{R} = 0.36[1 - \exp(-3.08(Ca)^{0.54})]$$

Bretherton [1961]

$$\frac{\delta}{R} = 1.34(Ca)^{2/3}$$

Aussilous and Quere [2000]

$$\frac{\delta}{R} = \frac{1.34(Ca)^{2/3}}{1 + 2.5(1.34(Ca)^{2/3})}$$

Han & Shikazono [2010]

$$\frac{\delta}{R} = 2.\left(\frac{0.968.Ca^{2/3}Bo^{-0.414}}{1 + 4.838Ca^{2/3}Bo^{-0.414}}\right)$$

Fig. 8. Comparison of the empirical scaling correlations for predicting the initial film thickness laid down by a moving meniscus inside a tube.

Table 1
Comparison of initial film thickness*.

BC	T_e (°C)	T_c (°C)	*Ca*	*Bo*	δ_0 → Eq. (8) (μm)	δ_0 → Section 3.2 (μm)
#1	46	16	0.0198	1.452	93.1	75
#2	46	20	0.0210	1.720	90.1	69
#3	46	24	0.0175	1.782	81.7	67

* Values of average *Ca* and *Bo* are calculated at mean temperature of T_e and T_c.

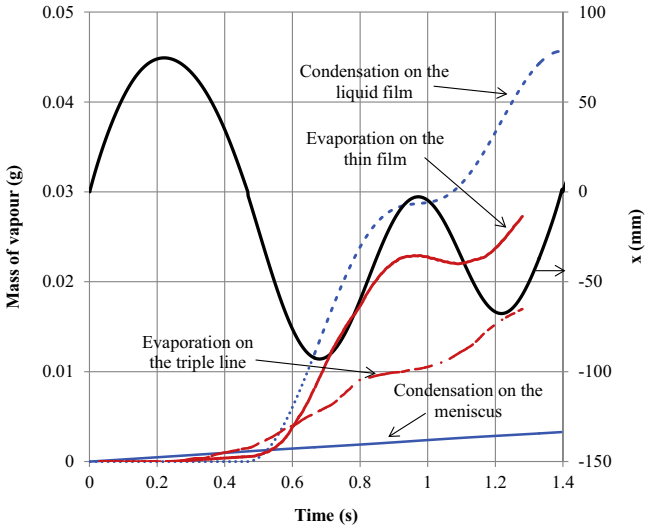

Fig. 9. Cumulated variation of vapour mass during one cycle, separating the four different contributions, as highlighted: Evaporation on the triple-line, or on the liquid film in the evaporator, and condensation on the liquid film, or on the meniscus in the condenser ($T_e = 46$ °C and $T_c = 16$ °C, first cycle).

to the amount of condensation on the liquid film. This latter component of condensation, which is due to the large variation of the liquid film length in the condenser, is much more critical and important. When the condenser section is full of liquid, its contribution is equal to zero, while it is maximum when the meniscus is at the bottom of the condenser section. The evaporation process is more complicated. Fig. 9 shows that the amount of vapour generated at the triple-line is significant and equal to more than 1/3 of the contribution of the liquid film evaporation. Furthermore, the evaporation rate at the triple-line can almost be considered as constant during the entire life of the liquid film while the evaporation on the liquid film is highly dependent on the location of the meniscus inside the tube. The net evaporation rate is maximum when the meniscus is at the bottom of the condenser, while it tends to zero or become slightly negative (i.e., condensation occurs on it) when the vapour is being compressed by the upward moving meniscus.

4. Summary and conclusions

Self-sustained thermally driven oscillations of a single meniscus can be obtained and efficiently sustained inside a capillary tube over long periods of time by maintaining a step thermal gradient over its length. Associated phase-change processes lead to thermo-mechanical instability in the system which generates continuous auto-oscillations of the meniscus. The amplitude of the oscillations not only depends on the temperature difference between the condenser and the evaporator, but also on their absolute temperature levels. Oscillations are quasi-periodic in nature for a range of imposed temperature gradients; they become more regular and periodic as this gradient decreases. In line with the

recent literature (by this group of authors and others), maximum pressure in the vapour space does not occur when the liquid meniscus is at top of evaporator section; it occurs when the meniscus reaches the adiabatic section in the downward stoke while going from the evaporator to the condenser. During this downward motion of the meniscus, a liquid film is laid down on the tube wall and the very high net evaporation rate of this film contributes to rapid increase of the pressure in the vapour space.

The two processes of evaporation and condensation of vapour to/from the liquid film and the meniscus respectively, may occur simultaneously during parts of the cycle. Net vapour mass flux is determined from the dominant mechanism out of these two. Condensation of vapour mostly occurs on the liquid film inside the condenser section. A small amount of condensation is also observed on the moving meniscus. For a given boundary condition, the film thickness and its length at a given time determines the overall dynamics of the meniscus. The results show that evaporation takes place at both, the triple-line and the liquid film interface, the continuation of the former mechanism being somewhat higher than the latter. The amount of vapour generated at the triple-line is significant and equal to more than $\sim$1/3 of the contribution of the liquid film evaporation. At the triple-line, the evaporation rate is nearly constant during one complete cycle, while it depends strongly on the location of the meniscus inside the system for the liquid film evaporation. With average value of Capillary and Bond numbers, the initial film thickness estimated by Han and Shikazono empirical correlation [29], is in the range 80–90 μm. This is in reasonable agreement with the range predicted by our present model (65–75 μm).

Most of the existing mathematical models fall short of predicting the entire thermo-hydrodynamics of pulsating heat pipes. While some do not include evaporation and condensation processes, others do not appreciate the dominant role of the liquid film in obtaining self-sustained oscillations. The intricate dependency of the net vapour pressure on simultaneous occurrence of evaporation and condensation is also not included by any of the models reported till date. Too, the occurrence of superheated vapour and the possibility of the existence of metastable phase behaviour need further exploration. The experiments reported here helps in understanding these critical issues and will contributed towards improved mathematical modelling of the entire PHP systems. Nevertheless, a predictive theoretical model of both the triple line and thin film evaporation is not easy to develop. It has to include the thermal inertia effects in both, the wall and the liquid film, respectively, as the thermal problem is highly non-stationary. Furthermore, the physics of the triple line – that has been widely studied in the literature – includes several unknown parameters which need to be taken into account (e.g., accommodation coefficient, disjoining pressure, contact angle).

Conflict of interest

None declared.

Acknowledgments

Financial support from the Indo-French Centre for the Promotion of Advanced Research (IFCPAR/CEFIPRA), New Delhi (Project #: IFCPAR: 4408-1/2010), under the aegis of Indian Department of Science and Technology and the French Ministry of Foreign Affairs is gratefully acknowledged. Especially, part of this article was written during the scientific visit of Prof. Lefèvre to IIT Kanpur and Prof. Sameer Khandekar to CETHIL, both with financial support of IFCPAR/CEFIPRA. This work was also supported by the French National Research Agency ANR in the frame of the TDM-AAP project 'AARDECO'.

References

[1] Y. Zhang, A. Faghri, Advances and unsolved issues in pulsating heat pipes, Heat Transfer Eng. 29 (1) (2008) 20–44.
[2] S. Khandekar, P.K. Panigrahi, F. Lefèvre, J. Bonjour, Local hydrodynamics of flow in a pulsating heat pipe: a review, Front. Heat Pipes 1 (023003) (2010) 1–20.
[3] L.L. Vasiliev, Heat pipes in modern heat exchangers, Appl. Therm. Eng. 25 (2005) 1–19.
[4] S. Rittidech, S. Wannapakne, Experimental study of the performance of a solar collector by closed-end oscillating heat pipe, Appl. Therm. Eng. 27 (11–12) (2007) 1978–1985.
[5] S. Khandekar, V. Silwal, A. Bhatnagar, P. Sharma, Global effectiveness of pulsating heat pipe heat exchangers: modelling and experiments, Heat Pipe Sci. Technol. – Int. J. 1 (3) (2010) 279–302.
[6] M. Arab, M. Soltanieh, M.B. Shafii, Experimental investigation of extra-long pulsating heat pipe application in solar water heaters, Exp. Therm. Fluid Sci. 42 (2012) 6–15.
[7] Y. Maydanik, V.I. Dmitrin, V.G. Pastukhov, Compact cooler for electronics on the basis of a pulsating heat pipe, Appl. Therm. Eng. 29 (2009) 3511–3517.
[8] H. Akachi, Structure of a heat pipe. U.S. Patent, Patent Number 4921041, 1990.
[9] H. Akachi, L-type heat sink. U.S. Patent, Patent Number 5490558, 1996.
[10] S. Rittidech, P. Terdtoon, M. Murakami, P. Kamonpet, W. Jompakdee, Correlation to predict heat transfer characteristics of a closed-end oscillating heat pipe at normal operating condition, Appl. Therm. Eng. 23 (2003) 497–510.
[11] Y. Zhang, A. Faghri, Heat transfer in a pulsating heat pipe with open end, Int. J. Heat Mass Transfer 45 (2002) 755–764.
[12] Y. Zhang, A. Faghri, M.B. Shafii, Analysis of liquid–vapour pulsating flow in a U-shaped miniature tube, Int. J. Heat Mass Transfer 45 (2002) 2501–2508.
[13] R.T. Dobson, Theoretical and experimental modelling of an open oscillatory heat pipe including gravity, Int. J. Therm. Sci. 43 (2) (2004) 113–119.
[14] R.T. Dobson, An open oscillatory heat pipe water pump, Appl. Therm. Eng. 25 (4) (2005) 603–621.
[15] V.S. Nikolayev, A dynamic film model of the pulsating heat pipe, J. Heat Transfer 133 (8) (2011) 081504.
[16] V.S. Nikolayev, Towards predictive modelling of pulsating heat pipes, Proc. 16th International Heat Pipe Conference, INSA Lyon, Lyon, France, 2012.
[17] M. Mameli, M. Marengo, S. Khandekar, Towards quantitative validation of a closed loop pulsating heat pipe numerical model, Proc. 16th International Heat Pipe Conference, 2012. Invited lecture.
[18] M. Mameli, M. Marengo, S. Zinna, Numerical model of a multi-turn closed loop pulsating heat pipe: effects of the local pressure losses due to meanderings, Int. J. Heat Mass Transfer 55 (2012) 1036–1047.
[19] R. Senjaya, T. Inoue, Oscillating heat pipe simulation considering bubble generation. Part I: Presentation of the model and effects of a bubble generation, Int. J. Heat Mass Transfer 60 (2013) 816–824.
[20] A.K. Bajpai, S. Khandekar, Thermal transport behaviour of a liquid plug moving inside a dry capillary tube, Heat Pipe Sci. Technol. 3 (2–4) (2012) 97–124.
[21] A. Majumder, B. Mehta, S. Khandekar, Local Nusselt number enhancement during gas–liquid Taylor bubble flow in a square mini-channel: an experimental study, Int. J. Therm. Sci. 66 (2013) 8–18.
[22] B. Mehta, S. Khandekar, Taylor bubble-train flows and heat transfer in the context of pulsating heat pipes, Int. J. Heat Mass Transfer 79 (2014) 279–290.
[23] B. Mehta, S. Khandekar, Measurement of local heat transfer coefficient during gas–liquid Taylor bubble train flow by infrared thermography, Int. J. Heat Fluid Flow 45 (2014) 41–52.
[24] S.P. Das, V.S. Nikolayev, F. Lefèvre, B. Pottier, S. Khandekar, J. Bonjour, Thermally induced two-phase oscillating flow inside a capillary tube, Int. J. Heat Mass Transfer 53 (19–20) (2010) 3905–3913.
[25] F. Bonnet, P. Gully, V. Nikolayev, Experimental study of a single branch cryogenic pulsating heat pipe: first results, Proc. Eurotherm Sem. on Gravitational Effects on Liquid–Vapour Phase Change, IUSTI, Hyeres, France, 2011.
[26] P. Gully, F. Bonnet, V. Nikolayev, N. Luchier, T.Q. Tran, Evaluation of the vapour thermodynamic state in PHP, Proc. 17th International Heat Pipe Conference, IIT Kanpur, Kanpur, India, 2013.
[27] S. Khandekar, Thermo-hydrodynamics of closed loop pulsating heat pipes (Ph.D. thesis) (available at: <http://elib.uni-stuttgart.de/opus/volltexte/2004/1939/>), 2004.
[28] M. Rao, F. Lefèvre, S. Khandekar, J. Bonjour, Understanding transport mechanism of a self-sustained thermally driven oscillating two-phase system in a capillary tube, Int. J. Heat Mass Transfer 65 (2013) 451–459.
[29] Y. Han, N. Shikazono, The effect of bubble acceleration on the liquid film thickness in micro tubes, Int. J. Heat Fluid Flow 31 (4) (2010) 630–639.